Journal of Sedimentary Research

Journal of Sedimentary Research, 2010, v. 80, 480–491
Research Article
DOI: 10.2110/jsr.2010.048

ESTIMATING THE OXYGEN ISOTOPIC COMPOSITION OF EQUATORIAL PRECIPITATION DURING THE MID-CRETACEOUS

MARINA B. SUAREZ,[1]* LUIS A. GONZÁLEZ,[1] AND GREGORY A. LUDVIGSON[2]
[1]*Department of Geology, The University of Kansas, 1475 Jayhawk Boulevard, Lawrence, Kansas 66045, U.S.A.*
[2]*Kansas Geological Survey, 1930 Constant Avenue, Lawrence, Kansas 66047, U.S.A.*
e-mail: msuarez5@jhu.edu

ABSTRACT: **Recent studies utilize the oxygen isotopic composition of pedogenic carbonates (siderite and calcite) to evaluate empirically the global hydrologic cycle during the Cretaceous. Pedogenic carbonates are used as a proxy for the isotopic composition of meteoric waters in order to estimate precipitation rates in the Aptian–Albian via a mass-balance model. These modeling studies have previously been limited to mid-latitude to high-latitude data, and thus a more extensive latitudinal data set is needed to produce a more globally constrained model.**

This study provides an equatorial (~ 2° S paleolatitude) data set from pedogenic sphaerosiderites of the Caballos Formation from the Upper Magdalena Valley, Colombia. In addition, macroscopic and microscopic morphological features of paleosols were used to identify ancient soil conditions. The gleyed appearance and presence of sphaerosiderites suggest that soils were dominated by water-saturated conditions, with occasional incursions of marine-influenced water resulting in pyrite precipitation. This observation constrains the sampling sites to paleoelevations near sea level. Paleosols are interpreted to have been Entisols, Inceptisols, and Ultisols similar to soils in coastal equatorial regions of modern Colombia. Relatively invariant $\delta^{18}O$ values and more variable $\delta^{13}C$ values produce vertical trends in $\delta^{13}C$ vs. $\delta^{18}O$ space called meteoric sphaerosiderite lines. The average oxygen isotopic composition for these trends is −4.41 ± 0.37‰ (VPDB). The average oxygen isotopic composition of meteoric waters precipitating the sphaerosiderites is estimated at −4.56 ± 0.38‰ (VSMOW). These are slightly more enriched than modern and modeled Cretaceous estimates of equatorial precipitation $\delta^{18}O$ but are generally in agreement with expected oxygen isotopic compositions of precipitation for this paleolatitude.

INTRODUCTION

The Cretaceous Period is a well-documented interval of global warmth and increased atmospheric moisture due to higher atmospheric concentrations of greenhouse gasses such as carbon dioxide (e.g., Barron and Moore 1994; Jenkyns et al. 2004; Poulsen 2004 and references therein). Average global temperatures are suggested to have been approximately six degrees higher than the modern global average (e.g., Barron and Moore 1994). However, while the importance of changes in the hydrologic cycle on global climate has been recognized for some time (Barron et al. 1989), only recently has it been the subject of rigorous investigations (Ludvigson et al. 1998; Hay and DeConto 1999; White et al. 2001; Ufnar et al 2002; Ufnar et al. 2004; Poulsen et al. 2007; Ufnar et al. 2008). Most authors hypothesize an intensified hydrologic cycle during the Cretaceous; for example, Barron et al. (1989) suggested increases in global precipitation between 18 to 22% relative to present day.

Ufnar et al. (2002) used paleoprecipitation $\delta^{18}O$ values calculated from isotopic values of pedogenic siderites in a simple isotope mass-balance model to estimate zonal precipitation rates during the mid-Cretaceous (Albian Stage). While both GCM simulations (e.g., Poulsen et al. 2007) and the Ufnar et al. (2002, 2004) mass-balance models indicate increased precipitation rates in the tropics and mid- to high latitudes, the Ufnar et al. (2002, 2004) estimates generally are higher, particularly in the mid- to high latitudes. For example, Ufnar et al. (2002) estimated zonal precipitation rate estimates at 45° N at 7.2 mm/day, while the GENESIS GCM estimates of Poulsen et al. (2007) are 4.0 mm/day. The mass-balance models simulate precipitation and evaporation fluxes during the poleward transport of atmospheric moisture from the equator, with an explicit goal of closely simulating the empirical $\delta^{18}O$ data from a wide range of paleolatitudes. The models of Ufnar et al. (2002, 2004) were constrained, however, by empirical data spanning only from 35° N to 75° N. Characterizing more complete ranges of Cretaceous latitudinal variations in $\delta^{18}O$ values of meteoric precipitation (i.e., full equator-to-pole trends) is critical to improve the precipitation estimates in the isotope mass balance models of Ufnar et al. (2002, 2004). Suarez et al. (2009) found that tropical isotopic compositions of meteoric precipitation are much lighter than those expected from the extrapolation of the paleogeographically limited 35° N to 75° N $\delta^{18}O$ trend of Ufnar et al. (2002). Moreover, the recent addition of a water isotope module to the GENESIS GCM, simulating water isotopic transport and fractionation effects (Poulsen et al. 2007) calls for further development of empirical $\delta^{18}O$ data sets for model calibration.

This study utilizes pedogenic sphaerosiderites from the Caballos Formation of Colombia to provide near-equator data expanding the range of our paleolatitudinal meteoric $\delta^{18}O$ transect from 75° N to 2° S.

* Present Address: Department of Earth and Planetary Sciences, Johns Hopkins University, 3400 North Charles Street, 301 Olin Hall, Baltimore, Maryland 21218, U.S.A.

 1527-1404/10/080-480/$03.00

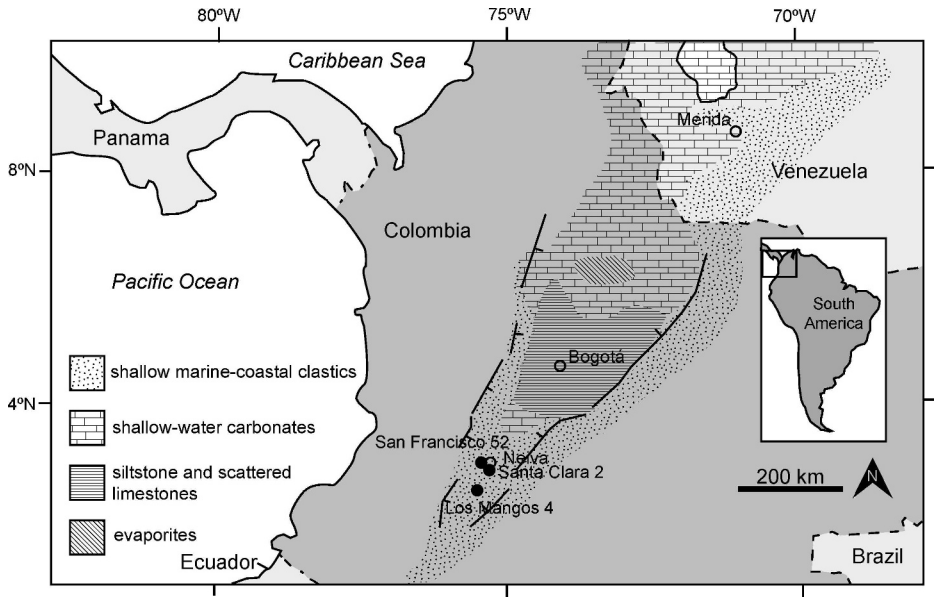

FIG. 1.—Location of cores and distribution of late Early Cretaceous facies in northwestern South America. Cores penetrating the Caballos Formation occur in the Neiva subbasin in the Upper Magdalena Valley of western Colombia (modified from Villamil et al. 1999).

Pedogenic sphaerosiderites are millimeter-scale spherulitic siderite nodules that form in wetland soils of variable drainage. The oxygen and carbon isotopic compositions of sphaerosiderites from a single paleosol often form linear trends called *meteoric sphaerosiderite lines* (MSLs) defined by relatively invariant oxygen isotopic values and more variable carbon isotopic values, and are interpreted to represent a shallow fresh groundwater system with relatively stable oxygen isotopic compositions (Ludvigson et al. 1998). These diagenetic trends can be used to determine the oxygen isotopic composition of meteoric water, in an application similar to that of *meteoric calcite lines* (Lohmann 1988; Ludvigson et al. 1998; White et al. 2000). The oxygen isotopic composition of meteoric calcite lines, and by extension MSLs, reflect the narrow range of precipitation $\delta^{18}O$, and despite seasonal variations, groundwater compositions are approximately equal to the average isotopic composition of mean annual precipitation (Allan and Matthews 1977, 1982; Lohmann 1988).

GEOLOGIC SETTING

The Caballos Formation, formally described by Corrigan (1967) (as cited in Vegara 1995) is dominated by sandstones and dark gray shales with coaly laminations transitioning to marine carbonates and has been interpreted to have formed in fluvial–estuarine environments (Villamil et al. 1999; Acevedo and Pennington 2003). The Caballos Formation was deposited in an extensional basin in what is now the Upper Magdalena River Valley region of Colombia (Fig. 1). Barrero et al. (2007) described the present-day Upper Magdalena Valley Basin as a "Neogene Broken Foreland" basin that evolved from the collision-related Paleogene foreland basin (Barrero et al. 2007). Guerrero et al. (2000) proposed the use of the term Cretaceous Colombian Basin to differentiate it from the compressional regime related basins that formed during the Paleogene and dominate the present-day Upper Magdalena Valley Basin. The Cretaceous Colombian Basin extended south into northernmost Ecuador and to the north into the open marine Maracaibo Basin of Venezuela. To the west the basin was bounded by the ancestral Central Cordillera and to the east the by the shorelines of the Guyana shield.

The Cretaceous rocks of northwestern to northern Colombia and northern Venezuela document an overall transgressive succession during the Aptian, with the lower to middle portions of the Caballos Formation representing the transition from fluvial deposits to fully marine deposits, and the upper sections documenting a regression during the Albian (Villamil et al. 1999; Guerrero 2002). The similarity between the depositional environments of the coal-bearing Caballos Formation with those of other mid-Cretaceous sphaerosiderite bearing formations (e.g., Ludvigson et al. 1998; Ufnar et al. 2001, 2002) led the authors to predict that sphaerosiderites would be present and probably abundant in portions of the Caballos Formation that were subject to subaerial exposure (interfluves) and paleosol development. Further investigation indicated the presence of well-developed paleosols and sphaerosiderites in the Caballos Formation.

METHODS

Core descriptions provided by the Litoteca Nacional de Colombia of the Instituto Colombiano de Petróleo (ICP), confirmed the presence of paleosols, and numerous sphaerosiderite-bearing horizons in several long drillcores penetrating the Caballos Formation in the Upper Magdalena River Valley. Sphaerosiderite-bearing horizons were sampled from seven cores housed at the Litoteca Nacional de Colombia, in Bucamaranga, Colombia (Table 1). A total of 61 resin-impregnated samples were sectioned to produce polished thin sections used for petrographic analysis and matching polished slabs for microsampling.

Thin sections were analyzed both to identify sphaerosiderites for isotopic analysis, to identify any late-diagenetic carbonates, and to generally evaluate paleosol micromorphology. Macroscopic and microscopic observations serve to provide qualitative evidence of depositional environment and soil conditions. Thin sections were analyzed using

TABLE 1.—*Cores, location, and number of samples from the Caballos Formation.*

Core	Latitude	Longitude	# of Samples
Los Mangos 4	2° 37′ 29.97″	−75° 33′ 33.05″	5
Los Mangos 7	2° 37′ 11.39″	−75° 32′ 47.93″	9
San Francisco 2	3° 4′ 58.49″	−75° 23′ 10.95″	8
San Francisco 52	3° 3′ 10.49″	−75° 24′ 16.53″	20
Santa Clara 2	2° 58′ 59.24′	−75° 21′ 2.92	6
Toy 2	3° 56′ 13.89″	−75° 19′ 34.26″	10
Toy 3	3° 57′ 33.14″	−75° 18′ 27.04′	3

plane-polarized and cross-polarized light on a Nikon SMZ1500 microscope fitted with an Optronics Magnafire SP digital camera and an Olympus BX51 microscope fitted with a Diagnostic Instruments SPOT Insight Firewire digital camera. In evaluating paleosol micromorphology, the fine-grained matrix (groundmass) and pedofeatures (coatings, mineral accumulations etc.) of the paleosols were described using terms from Stoops (2003). Clay minerals are described with respect to their birefringence fabric (b-fabric), which describes the pattern, orientation, and distribution of interference colors from the clay mineral crystals.

Through petrographic analysis, 15 horizons from three cores (San Francisco 52, Los Mangos 4, and Santa Clara 2) were identified that had un-oxidized or minimally oxidized sphaerosiderites that were large enough in diameter to produce 60 to 180 µg powdered samples. For some horizons, two or three sphaerosiderites were combined to produce one sample. Analyses were carried out at the W.M. Keck Paleoenvironmental and Environmental Stable Isotope Lab at the University of Kansas, and the Paul H. Nelson Stable Isotope Laboratory at the University of Iowa. Microsamples were extracted using a microscope-mounted dental drill fitted with 3 to 500 µm diameter tungsten-carbide bits. Microsamples (n = 119) were vacuum roasted at 200°C for one hour to remove volatile contaminants. Samples were digested at 75° C with 100% phosphoric acid in a ThermoFinnigan Kiel III single-sample acid dosing system connected to a dual-inlet ThermoFinnigan MAT 253 isotope-ratio mass spectrometer (University of Kansas), or Finnigan MAT 252 isotope-ratio mass spectrometer (University of Iowa). Precision was monitored by daily analysis of NBS-18 and NBS-19 and is better than 0.07‰ for oxygen and 0.03‰ for carbon, with all carbonate data being reported relative to VPDB. Siderite oxygen isotopic values were corrected to account for the temperature-dependent fractionation factor between phosphoric acid and siderite utilizing data in Carothers et al. (1988).

RESULTS

Macroscopic Features

The three cores examined in detail consist generally of meter-scale beds of gray mudstones, sandstones, and conglomerates. Approximately 1.25 m of stratigraphic section with sphaerosiderite-bearing horizons were sampled from the Los Mangos 4 core (Fig. 2), and 0.95 m from the Santa Clara 2 core (Fig. 2). Two sections from the San Francisco 52 core were sampled. The lower section was approximately 3.0 m long (Fig. 2), whereas the upper section was the longest section that was sampled at approximately 14 m (Fig. 3). A number of features described below provide evidence of depositional and soil-forming conditions.

Root Traces.—Root traces are abundant in all three cores examined. These features occur as sinuous, downward-branching black traces that range in diameter between a few millimeters to approximately 0.5 cm, and are as long as 8 cm. (Fig. 4A, B)

Burrows.—Burrows are common in the three cores, but are particularly evident in the San Francisco 52 core because they are mostly preserved as distinct Fe-oxide mineral accumulations that are very dusky red (5R2.5/2) to reddish black (5R2.5/1) and have sharp boundaries with the surrounding matrix (Fig. 4B). The burrows occur as interconnected networks that most often occur in association with root traces. More discrete sand-filled burrows also occur in the San Francisco 52 and the Los Mangos 4 cores. The burrow in the San Francisco 52 core is a branching burrow approximately 1 mm in diameter (Fig. 4C). The burrow in the Los Mangos 4 core is a vertical sand-filled burrow approximately 2.5 mm in diameter (Fig. 4J). Burrows from the Santa Clara 2 core are identified as *Paleophycus* and *Teichichnus* in ICP core logs.

Mottling.—Color mottles occur mainly in the upper section of the San Francisco 52 core between about 864 m and 862 m, and are associated with the root traces and Fe-oxide preserved burrows described in the previous sections. The mottles are weak red (5R4/2) and differ from the burrows in having diffuse boundaries with the surrounding matrix (Fig. 4B).

Microscopic Features

Thin sections of hand samples collected from the three cores were examined under plane-polarized, cross-polarized, and reflected light. Groundmass and other features are described below.

Groundmass.—The birefringence of the fine-grained components includes strial b-fabrics, speckled b-fabrics, and various morphologies of striated b-fabrics. The Los Mangos core is chiefly characterized by parallel-striated to cross-striated and granostriated b-fabrics which consist of zones or streaks of birefringent clays that form parallel, cross, or concentric patterns around quartz grains and sphaerosiderites (Fig. 4D, E). In more sandy horizons (e.g., 957.38 m) fine-grained portions consist of speckled b-fabrics consisting of smaller random domains of birefringent zones.

The fine-grained groundmass of the lower portion of the Santa Clara 2 core is characterized by strial b-fabric, consisting of thin layers of horizontally oriented clay layers that exhibit a uniform extinction with a speckled pattern (Fig. 4F). The upper horizon (799.22 m to 799.01 m) from the Santa Clara 2 core consists of a groundmass that is characterized by parallel-striated, cross-striated, and granostriated b-fabrics.

The mudstone horizons in the lower portion of the San Francisco 52 core consist of fine-grained groundmass characterized by parallel-striated, cross-striated. and granostriated b-fabrics. The upper, longer section of the San Francisco 52 contains horizons (873.18 m, 871.75 m, and 861.96 m to 860.08 m) that are characterized by speckled b-fabric to parallel-striated b-fabric. The remaining horizons (871.54 m to 871.45m and 867.32 m to 864.28 m) are characterized by parallel-striated, cross-striated, and granostriated b-fabrics.

Mineral Accumulations.—Mineral accumulations include siderite (predominantly in the form of sphaerosiderites), pyrite (mostly framboids), and Fe-oxide accumulations. From the Los Mangos 4 core, sphaerosiderites range from one to two millimeters in diameter, and have radiating crystallites that range from fibrous to thicker, bladed crystals. Some appear concentrically zoned, suggesting more than one period of crystal growth. Sphaeorsiderites in horizon 959.93 m are particularly cloudy and are enriched in pyrite inclusions relative to the surrounding matrix. These sphaerosiderites often have a thin outer rim of more clear radial crystals. The five samples from the Los Mangos core all have some pyrite framboids and/or pyritized organic material in the fine-grained matrix, and many sphaerosiderites have enveloped these pyrite crystals or have nucleated around pyrite (Fig. 4G). Sphaerosiderites are often oxidized along the rims or along fractures and between crystallites.

Sphaerosiderites approximately 0.2 to 0.7 mm in diameter, and consisting of radial-fibrous crystallites occur in horizons 799.22 m, 799.15 m, and 799.01 m of the Santa Clara 2 core. These sphaerosiderites have oxidized rims. Oxidized siderite crystals, less than 0.2 mm in diameter, occur in the sample at horizon 802.50 m. Minor amounts of pyrite occur in these samples, mainly in the lowest sample (802.52 m).

The bottom four samples of the lower portion of the San Francisco 52 core contain small sphaerosiderites approximately 0.2 mm in diameter or smaller with minor oxidation rims. The sample at horizon 894.04 m contains abundant pyrite framboids 0.02 to 0.03 mm in diameter. A few pyrite framboids are much larger, approximately 0.2 mm in diameter (Fig. 4H). A sandstone horizon at 893.73 m is cemented by microspar to

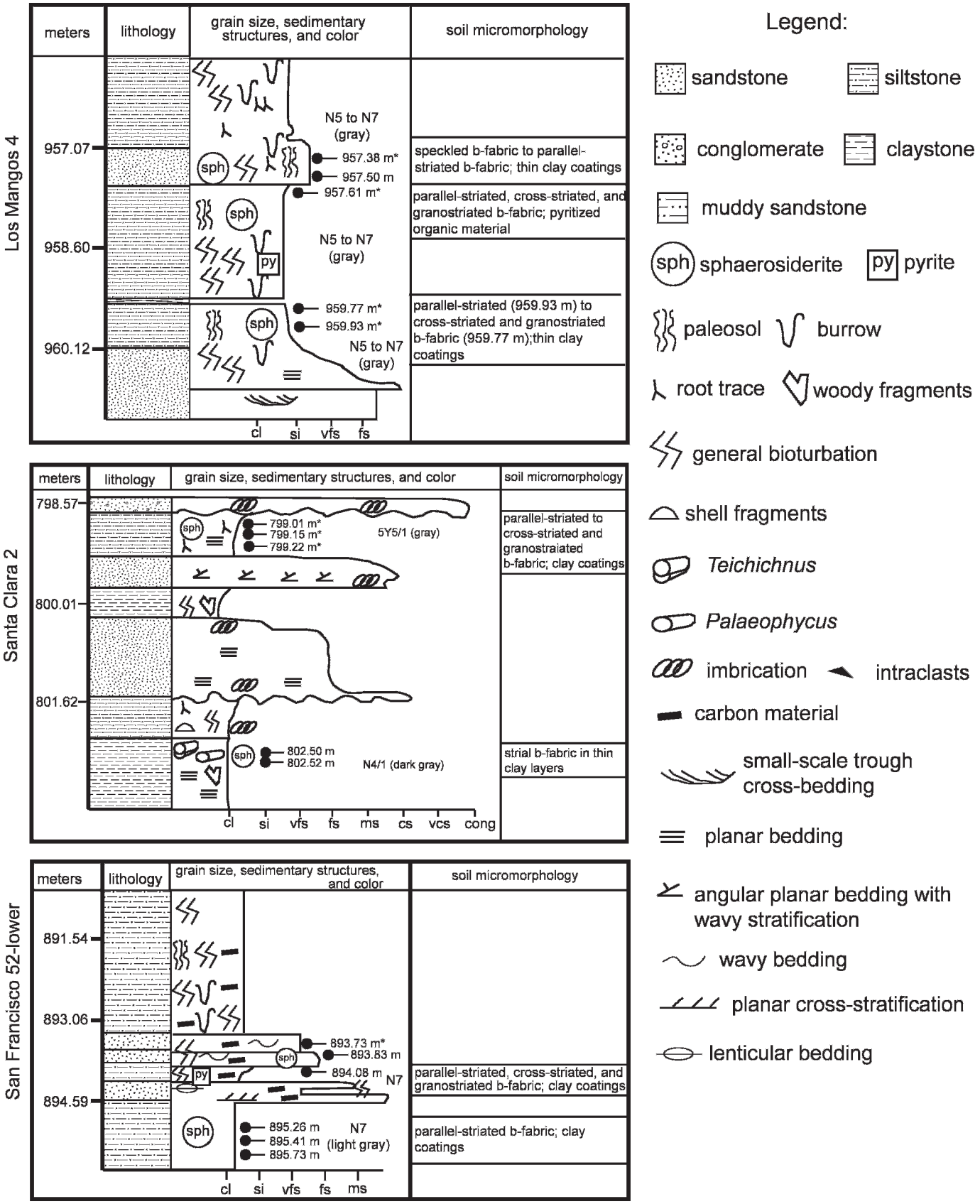

FIG. 2.—Lithology, grain size, sedimentary structures, and soil micromorphology from a section of the Los Mangos 4 core, the Santa Clara 2 core, and the lower portion of the San Francisco 52 core. Modified from Ecopetrol-ICP (1999, 2000a, b). Asterisks indicate isotopic analyses.

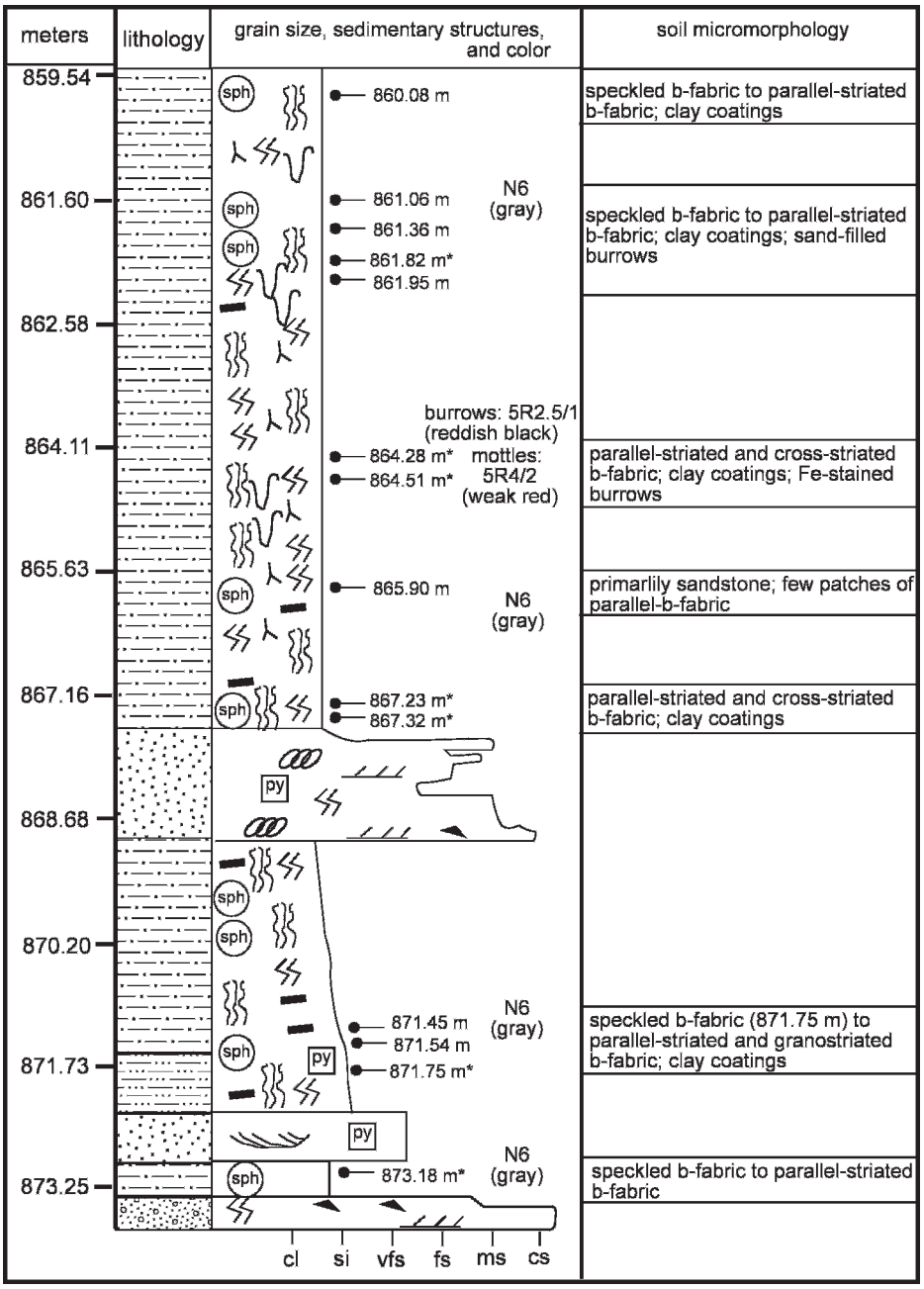

FIG. 3.—Lithology, grain size, sedimentary structures, and soil micromorphology from a section of the upper portion of the San Francisco 52 core. See Figure 2 for legend. Modified from Ecopetrol-ICP (2000b).

sparry, subhedral intergranular siderite, chalcedony, and minor amounts of calcite. The largest siderite spar crystals have dimensions of approximately 0.2 by 0.3 mm.

Sphaerosiderites in the upper section of the San Francisco 52 core generally consist of radial fibrous to bladed crystallites, and have diameters ranging from 0.4 mm to 1.0 mm. Sphaerosiderites often form in clusters, sometimes sinuous clusters (Fig. 4I). The majority of the samples contain pyrite framboids in the surrounding matrix. Some pyrite framboids are enveloped by the siderites. Sphaerosiderites from 860.08 m consist of microcrystalline cores, surrounded by a band of pyrite framboids, and an outer zone of radial fibrous siderite crystallites. Minor amounts of oxidation occur on rims of sphaerosiderites; however, somewhat more heavily oxidized rims of sphaerosiderites occur in regions where they are associated with iron-oxide preserved burrows. Some sphaerosiderites at 871.54 m and 871.75 m also appear to have a zone of pyrite growth.

Clay Coatings.—Clay coatings occur as highly birefringent domains of clay minerals lining voids or grains. In the Los Mangos 4 core, thin clay coatings occur around some quartz grains in the sample at 959.77 m, as well as in small voids of the sandy horizon at 957.50 m, and within a vertically oriented sand-filled burrow at 957.38 m (Fig. 4J).

Thicker, more developed clay coatings occur along and between sphaerosiderites in the Santa Clara 2 core, at horizons 799.22 m and 799.15 m (Fig. 4K). In addition, thin clay coatings occur along sinuous to irregular subhorizontal partings within the rock.

Mudstones in the lower portion of the San Francisco 52 core contain clay coatings along subhorizontal, sinuous partings within the rock. Sphaerosiderites occasionally occur associated with these partings and also have thin clay coatings. Clay coatings occur in most of the samples through the upper section of the San Francisco 52 core. As in the lower portion of the core, thin clay coatings occur along subhorizontal, sinuous

partings within the rock which often branch (Fig. 4L). Sphaerosiderites that occur in clusters or along these sinuous partings often have thin clay coatings (Fig. 4I). These clusters of sphaerosiderites are especially common in horizons 861.96 m to 861.06 m.

Stable Isotopes

Overall, the data for thirteen individual sphaerosiderite-bearing horizons consists of relatively invariant $\delta^{18}O$ values with highly variable $\delta^{13}C$ values. These trends in $\delta^{18}O$ vs. $\delta^{13}C$ space are defined as meteoric sphaerosiderite lines (MSLs) (Ludvigson et al. 1998). The thirteen sphaerosiderite-bearing horizons define thirteen individual MSLs (Table 2 and Fig. 5). The average $\delta^{18}O$ of each of the 13 horizons ranged from −3.91‰ to −5.23‰, with the $\delta^{13}C$ values ranging from −16.02‰ to −2.37‰.

One horizon at 959.93 m in the Los Mangos 4 core contained sphaerosiderites whose isotopic compositions did not produce a MSL, and had highly variable $\delta^{18}O$ and $\delta^{13}C$ values, and also had more negative $\delta^{18}O$ values than all of the other sphaerosiderites horizons. The siderite-cemented sandstone (San Francisco 52 893.73 m) produced variable $\delta^{18}O$ values (ranging from −7.82 to −10.54‰) and variable $\delta^{13}C$ values (ranging from −1.52 to −2.75‰).

INTERPRETATIONS

Depositional Setting and Paleosols

The Caballos Formation in the Upper Magdalena Valley consists of terrestrial strata that, according to ICP core interpretations (1999, 2000a, 2000b), are characterized by fluvial channels, passive-channel-fill and crevasse-splay deposits, and floodplain environments. Petrographic observations provided in this study offer additional important details regarding the ancient soil conditions of paleosols that formed in flood plains and overprinted channel fills and crevasse splays. Overall, the paleosols are characterized by gleyed colors (N7 to N6, light gray to gray), root traces (Fig. 4A, B), and sphaerosiderites. Sphaerosiderites form principally in the phreatic zone, under reducing conditions in water-saturated soils (Ludvigson et al. 1998). The overall gleyed appearance of the soils also indicates waterlogged conditions (Birkeland 1999). The presence of iron-oxide cemented burrows, weak red mottles that represent redoximorphic conditions, and clay coatings suggests, however, that sometime during their formation some of the soil conditions transitioned from saturated, reduced conditions to moderately well-drained conditions, above the water table (vadose zone), where more oxidizing conditions and clay illuviation occurred (McCarthy et al. 1999; Birkeland 1999; Ufnar et al. 2001). In addition, the birefringence fabrics that occur in the fine-grained groundmass occur due to pressure and tension of the clays often due to wetting and drying of the soil and/or bioturbation (Brewer 1964; Retallack 1997; Stoops 2003).

The presence of pyrite framboids suggests that the paleosols were occasionally influenced by sulfate-bearing waters. Influence by marine or mixed marine–freshwater fluids (salinities ranging from $>$ 0.5 ppt to 30 ppt) is consistent with the fluvial–estuarine interpretations by previous authors (Villamil et al. 1999; Acevedo and Pennington 2003). The addition of sulfate-rich waters to organic-rich sediments where organic-matter degradation has evolved to anoxic conditions results in sulfate reduction, releasing sulfide that reacts with available reduced iron and quickly precipitates pyrite (Curtis and Coleman 1986). Most paleosols are characterized by pyrite that precipitated early during soil formation or before active pedogenesis occurred. This is suggested by siderites that have nucleated around pyrite or enveloped pyrite that was present in the matrix during their growth. Siderite began to precipitate as the source of sulfate was removed and/or sulfate was depleted and organic matter-degradation progressed to the methanogenic phase (Gautier and Claypool 1984). Some soils appear to have multiple phases of pyrite and siderite precipitation. These alternations between pyrite and siderite growth indicate that local base-level oscillation, lateral progradation/retrogradation of the shoreline, or even prolonged storm surges influenced the pore-water chemistry such that sulfate availability was the principal factor in precipitation of either pyrite or siderite as the presence of sulfide inhibits the precipitation of siderite in favor of pyrite (Heese 1990; Ludvigson et al. 1996; Ufnar et al. 2001). Multiple generations of siderite growth may account for the variation, though small, in $\delta^{18}O$.

Detailed descriptions for paleosols of each core are given below. When possible, paleosols are classified following USDA soil taxonomy nomenclature (Soil Taxonomy 1999) and aided by petrographic characteristics as described in Retallack (1997).

Los Mangos 4 Core.—The lower fining-upward section between 960.12 m and 957.61 m (Fig. 2) are claystones which have parallel-striated, cross-striated, and granostriated b-fabrics that are indicative of soil development that includes wetting and drying, bioturbation due to roots and soil organisms, and displacement of clay by the well-developed sphaerosiderites (Figs. 4D, G). The ancient soil conditions were dominated by water-saturated conditions, though thin clay coatings represent clay illuviation and a change to moderately well-drained conditions. Well-drained conditions in the paleosol were not prevalent, inasmuch as there are no redoximorphic features associated with the soil. The break in rock recovery just above 959.77 m might suggest that this interval represents two paleosols, both of which resemble weakly developed Ultisols, in that there are high clay contents (argillic or kandic horizons) and no weatherable minerals such as feldspars. The pyrite is an early diagenetic feature of the parent material, based on the observation that some sphaerosiderites (e.g., 957.61 m) nucleated around pyrite framboids (Fig. 4G), suggesting a drop in base level to bring the sedimentary material into the zone of pedogenesis.

The paleosol represented by the upper two samples of the Los Mangos 4 core are sandstones or clayey sandstones and have speckled b-fabric to parallel-striated b-fabric. Like the lower sample, pyrite occurred as an early diagenetic product of the influence of sulfate-rich water in the parent material. A base-level drop would have brought the parent material into the zone of active pedogenesis. Small relict cross-beds are present in the uppermost sample suggesting poorly developed paleosols; however, thin clay coatings represent some translocation of clays (Fig. 4J), indicating that this paleosol can be interpreted as an Inceptisol.

Santa Clara 2 Core.—The lower two samples (802.52 m and 802.50 m) (Fig. 2) are silty mudstones to fine sandstones with horizontal bedding and no evidence of pedogenesis, suggesting that this portion of the core is not a paleosol (Fig. 4F). In addition, *Teichichnus* and *Paleophycus* are often associated with subaqueous, often estuarine conditions. The ichnofauna, along with the minor amounts of pyrite, would suggest deposition in an estuarine environment that transitioned to saturated freshwater conditions marked by the formation of small siderite crystals in horizon 802.50 m.

The paleosol represented by samples at 799.01 m, 799.15 m, and 799.22 m is characterized by cross-striated to granostriated b-fabrics (Fig. 4E) and thicker clay coatings, (Fig. 4K) and does not contain weatherable minerals. These features are consistent with an interpretation of the paleosol as an Ultisol. Soil conditions transitioned from saturated to more well-drained conditions, resulting in translocation and formation of clay coatings and the slight oxidation of sphaerosiderites (McCarthy and Plint 1998; McCarthy et al. 1999). The soil maintains its overall gleyed (2.5Y6/1 to 2.5Y5/1, gray) appearance throughout, suggesting that periods of well-drained conditions were short; however, additional features such as evidence of redoximorphic conditions may have been

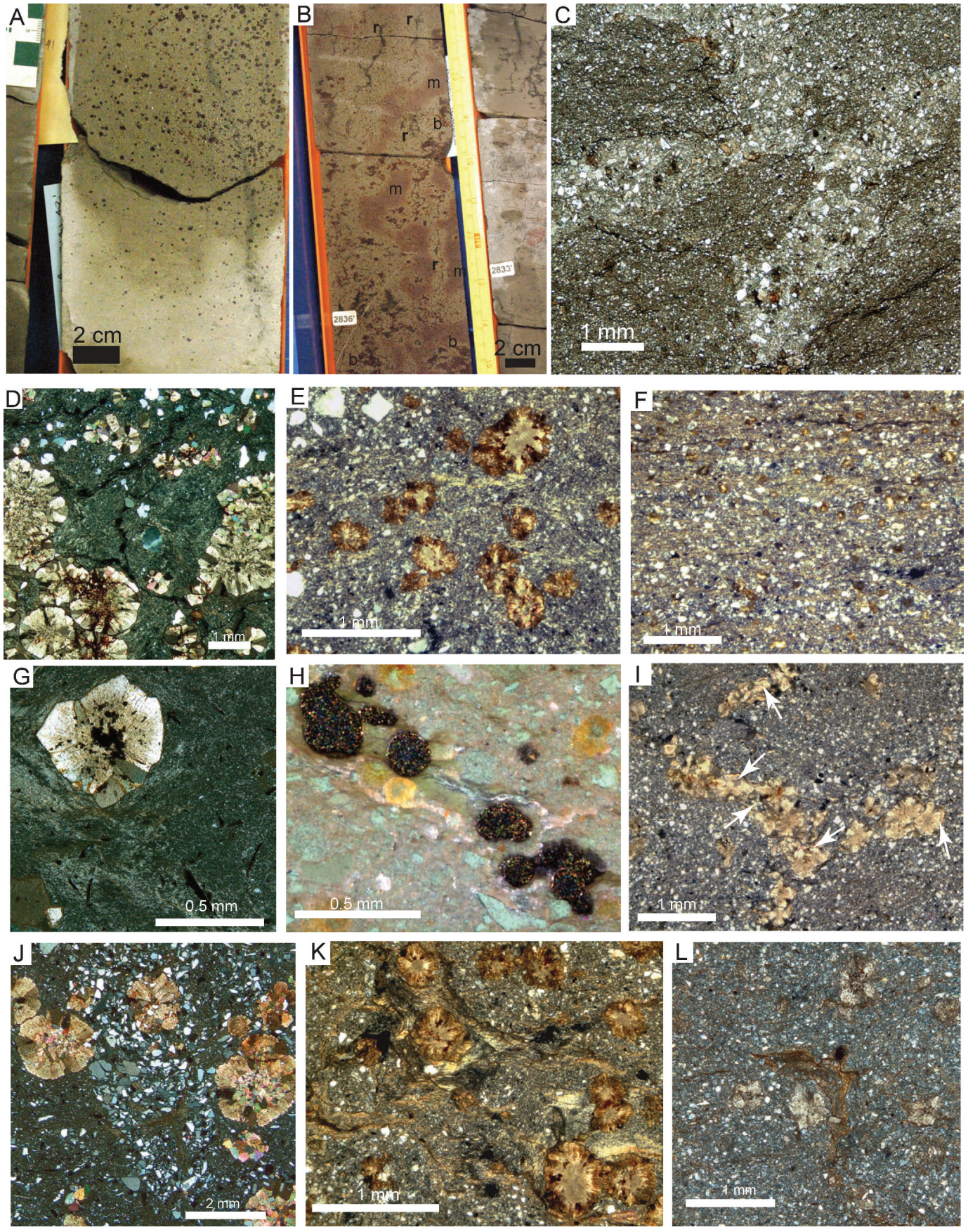
A
2 cm
B
r
r
m
b
r
m
r
m
2836'
2833'
b
b
2 cm
C
1 mm
D
1 mm
E
1 mm
F
1 mm
G
0.5 mm
H
0.5 mm
I
1 mm
J
2 mm
K
1 mm
L
1 mm

TABLE 2.—*Average $\delta^{18}O$, standard deviation, and range of $\delta^{13}C$ of meteoric sphaerosiderite lines from the Caballos Formation.*

Core	Horizon	$\delta^{18}O$ (avg. ± St.Dev., VPDB)	$\delta^{13}C$ (range, VPDB)
Los Mangos 4	957.38 m (3141.00 ft)	−4.75‰ 0.52‰	−14.41‰ to −16.02‰
	957.61 m (3141.75 ft)	−3.91‰ 0.47‰	−13.01‰ to −13.90‰
	959.77 m (3148.85 ft)	−3.92‰ 0.38‰	−9.51‰ to −12.15‰
Santa Clara 2	799.01 m (2621.42 ft)	−4.32‰ 0.12‰	−1.82‰ to −5.72‰
	799.15 m (2621.88 ft)	−4.60‰ 0.13‰	−13.79‰ to −15.04‰
	799.22 m (2622.11 ft)	−4.55‰ 0.11‰	−10.82‰ to −13.94‰
San Francisco 52	861.82 m (2827.50 ft)	−4.39‰ 0.09‰	−5.33‰ to −8.17‰
	864.28 m (2835.58 ft)	−4.70‰ 0.48‰	−7.60‰ to −14.01‰
	864.51 m (2836.33 ft)	−5.23‰ 0.72‰	−9.64‰ to −12.89‰
	867.23 m (2845.25 ft)	−4.17‰ 0.51‰	−2.13‰ to −4.15‰
	867.32 m (2845.54 ft)	−4.32‰ 0.80‰	−2.37‰ to −4.62‰
	871.75 m (2860.08 ft)	−4.48‰ 0.21‰	−7.80‰ to −8.99‰
	873.18 m (2864.75 ft)	−3.96‰ 0.22‰	−2.24‰ to −9.28‰

eroded because the thin nature of the soil horizon and the erosional contact with the overlying channel sandstone suggests truncation.

San Francisco 52 Core.—In the lower portion of the San Francisco 52 core (Fig. 2), the mudstone horizon from approximately 895.73 m to 894.59 m is characterized by parallel-striated b-fabrics and small sphaerosiderites. Thin subhorizontal clay coatings along partings are interpreted as root traces. This paleosol likely represents an immature soil, possibly an Inceptisol. A thin mudstone exists between two sandstones that overlie the paleosol (894.08 m). The sample from this mudstone exhibits parallel-striated to cross-striated and granostriated b-fabrics, small sphaerosiderites, and thin clay coatings, and also resembles an Inceptisol. An interesting feature of this horizon is the presence of large pyrite framboids (up to 0.2 mm in diameter) throughout the matrix and smaller ones within some sphaerosiderites (Fig. 4H). These larger pyrite framboids may suggest a later more sustained period of sulfate-rich water under reducing conditions.

The upper and longer portion of the San Francisco 52 core contains multiple paleosols (Fig. 3). The lowermost sample (873.18 m) is characterized by speckled b-fabric with small areas containing parallel-striated b-fabrics. This horizon is also characterized by large sphaerosiderites, some of which have coalesced into siderite-cemented patches, and thin clay coatings. The paleosol is interpreted as an Inceptisol

The three samples from approximately 871 m are at the base of a much thicker paleosol. The paleosol has an overall gleyed (N6 to N7) appearance suggesting that water-saturated conditions were prevalent. The paleosol is characterized by speckled b-fabric at the base, and parallel-striated to granostriated in the upper two samples. Thin clay coatings along sinuous subhorizontal partings are interpreted as root traces. In addition, the siderites at 871.75 m are more abundant and larger than those of the two samples above. This is most likely a result of these siderites residing in the reduced waters of the saturated zone for periods longer than those above. The overlying samples have better preserved thin clay coatings, suggesting that slightly more well-drained conditions were more frequent higher in the soil. Sphaerosiderites in the lower two samples (871.75 m and 871.54 m) have a concentric zone in which small pyrite framboids are abundant, indicating a temporary incursion of sulfate-rich waters. The soil represented by this paleosol was likely an Inceptisol.

The upper 9 m of mudstone we interpret as stacked paleosols, possibly representative of cumulative soil formation. The horizon at 864 m contains abundant redoximorphic features represented by reddish iron oxides concentrated within burrows or as mottles and throughout the paleosol (Fig. 4B). These features represent seasonally fluctuating water tables and better drained soil conditions than those in the more hydromorphic soils described above. Sphaerosiderites are commonly associated with sinuous clay coatings along root traces (Fig. 4I, L). The sphaerosiderites also have clay coatings suggesting changes in saturation and drainage resulting in clay illuviation. The branching sand-filled burrows (Fig. 4C) and Fe-stained interconnected burrows (Fig. 4B) resemble those attributed to either ants or termites. Both insects produce interconnected chambers and galleries that often form a grid-like lattice, and would have produced the burrows during periods in which soils were above the water table (Hasiotis 2006). A change in saturation from oxidized to reducing conditions is indicated by the fact that sphaerosiderites crosscut many of the Fe-oxide stains and concentrations. The dominance of gleyed colors (N6) and the generally un-oxidized state of sphaerosiderites indicate that hydromorphic features subsequently

←

FIG. 4.—Photographs and photomicrographs of root traces, burrows, birefringence fabrics (b-fabrics), mineral accumulations, and clay coatings. **A)** Photograph at 957.38 m of the Los Mangos 4 core showing a root trace (black vertical feature) and millimeter-scale sphaerosiderites (dark red spherical nodules). Scale bar = 2 cm. **B)** Photograph of the San Francisco 52 core at 864.41 m showing root traces (black features marked "r"), redoxomorphic color mottles (red patches marked "m"), and red-stained burrows (marked "b"). Scale bar = 2 cm. **C)** Photomicrograph (plane-polarized light) of a sand-filled burrow from the San Francisco 52 core, horizon 861.06 m. Scale bar = 1 mm. **D)** Photomicrograph (cross-polarized light) of the horizon at 959.77 m of the Los Mangos 4 core showing cross-striated b-fabric (bright streaks of clay minerals within the clay matrix forming a cross pattern) to granostriated b-fabric (bright streaks of clay minerals around quartz grains and/or sphaerosiderites). Scale bar = 1 mm. **E)** Photomicrograph (cross-polarized light) of dominantly parallel-striated b-fabric (streaks of clay oriented parallel to each other) to granostriated b-fabric in horizon at 799.15 m of the Santa Clara 2 core. Scale bar = 1 mm. **F)** Photomicrograph (cross-polarized light) of strial b-fabric (preferred parallel orientation that becomes extinct when rotated) in horizon at 802.50 m of the Santa Clara 2 core. Scale bar = 1 mm. **G)** Photomicrograph (cross-polarized light) of a sphaerosiderite with pyrite nuclei and flecks of pyritized organic material (opaque material) in the Los Mangos 4 core, horizon at 957.61 m. Note also the granostriated b-fabric. Scale bar = 0.5 mm. **H)** Photomicrograph of large pyrite framboids from the San Francisco 52 core, horizon 894.08 m taken under transmitted and reflected light. Scale bar = 0.5 mm. **I)** Photomicrograph (cross-polarized light) of a sinuous cluster of sphaerosiderites with thin clay coatings (arrows) at horizon 861.63 m of the San Francisco 52 core. Scale bar = 1 mm. **J)** Photomicrograph (cross-polarized light) showing a sand-filled vertical burrow with crescent-shaped clay coating from the Los Mangos 4 core, horizon 957.38 m. Scale bar = 2 mm. **K)** Photomicrograph (cross-polarized light) clay coatings along sphaerosiderites and subhorizontal partings in the Santa Clara 2 core, horizon 799.15 m. Scale bar = 1 mm. **L)** Photomicrograph (cross-polarized light) of a sinuous, branching parting with clay coating from the San Francisco 52 core, horizon 860.08 m. Scale bar = 1 mm.

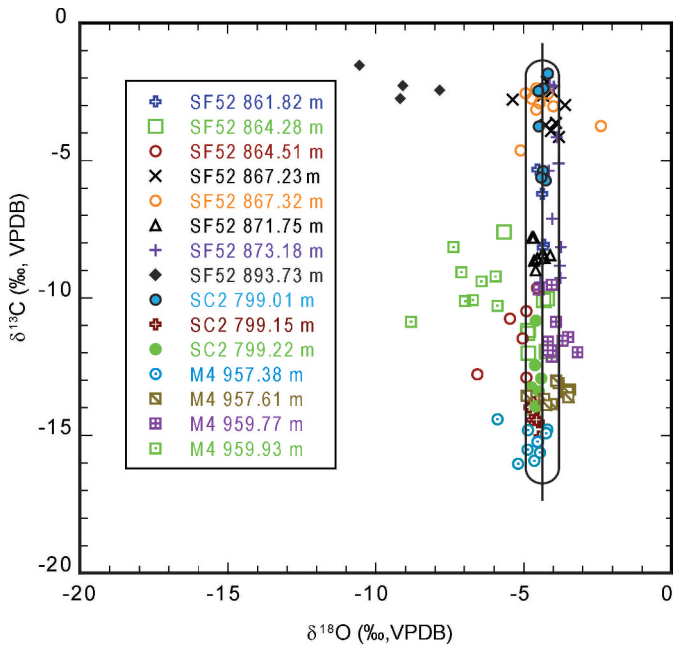

FIG. 5.—Plot of $\delta^{18}O$ vs. $\delta^{13}C$ for sphaerosiderites from the Caballos Formation. Vertical line is positioned at the average $\delta^{18}O$ composition (−4.36‰) of all meteoric sphaerosiderite lines, and rounded rectangle depicts the standard deviation (0.55‰).

dominated the soils. The lack of weatherable minerals, the abundance of clay coatings, the accumulation of redoximorphic features, and the presence of cross-striated b-fabrics suggest that these paleosols were similar to modern Ultisols. Sandier horizons (865.90 m) that are characterized by speckled b-fabrics (861.95 m to 860.08 m) may represent Inceptisols. The upper horizon, especially the sample at 860.08 m, contains sphaerosiderites characterized by concentric bands of pyrite framboids within the nodules, recording the temporary influence of sulfate-rich waters.

Estimate of Paleogroundwater Isotopic Composition

The average oxygen isotopic compositions of the sphaerosiderites at each horizon that define unique MSLs can be used to calculate the compositions of the groundwaters from which they were precipitated. To do this, we utilized the temperature-dependent fractionation equation for siderite from Carothers et al. (1988), and a zonal paleotemperature estimate based on data from Cretaceous leaf physiognomy of Wolfe and Upchurch (1987) and Spicer and Corfield (1992) as reported by Ufnar et al. (2002), in which t = temperature in °C, and l = latitude.

$$t = 30.25 - 0.2025 \times l - 0.0006 \times l^2 \quad (1)$$

During the Aptian–Albian, northern South America was located just south of the paleoequator (Meschede and Frisch 1998; Villamil et al. 1999). Using a paleolatitude of 2° S for the Caballos Formation, the mean annual temperature during the formation of sphaerosiderites in paleosols is estimated at approximately 30°C. The oxygen isotopic compositions of groundwaters calculated from the meteoric sphaerosiderite lines are summarized in Table 3. The average oxygen isotopic composition of groundwater determined by MSLs from the Caballos Formation is −4.56 ± 0.38‰ (VSMOW). This composition reflects the oxygen isotopic composition of meteoric groundwater, and over the time-averaged span of soil formation, the isotopic composition of mean annual precipitation. While the presence of pyrite indicates the influence of marine fluids, these fluids did not contribute to the isotopic composition of siderite precipitation because no hyperbolic mixing trends are present in the $\delta^{18}O$ vs. $\delta^{13}C$ data as has been demonstrated for marine influenced siderite precipitation (Ufnar et al. 2004) or for calcites interpreted to be deposited under mixed marine–freshwater conditions (Suarez et al. 2009).

DISCUSSION

According to Guerrero et al. (2000) sediments making up the Caballos Formation were sourced mostly from the emerging highlands to the west of the basin and the paleosol bearing strata were deposited on a broad coastal deltaic to estuarine complex during the early stages of a major transgression (Villamil et al. 1999). The Cretaceous Colombian Basin was subject to frequent sea-level oscillation as indicated by alternating fluvial deposits and shallow marine to estuarine deposits in the Caballos Formation. Numerous paleosols attest to the repeated and sustained exposure of these sediments, while the common presence of pyrite in several sequences indicates reducing conditions in phreatic systems influenced by seawater or freshwater–seawater mixed fluids on a coastal plain near sea level. Despite this influence, the fact that no mixing lines between seawater compositions and freshwater compositions occur suggests that the oxygen isotopic compositions of freshwater fluids precipitating siderites were not influenced by more positive marine oxygen isotopic compositions.

The micromorphology of some paleosols of the Caballos Formation is characteristic of seasonally saturated soils that we interpret as Ultisols. These soils occur in warm, humid environments (Soil Taxonomy 1999) and are similar to modern soils that occur in lowlands of Colombia and Venezuela today and various other tropical regions in Africa, Asia, and the southeastern regions of the USA. These soils most likely developed during lowstands in the more distal parts (i.e., farther away from channels or estuary shoreline) of the fluvial–estuarine system where the Caballos sediments accumulated. The paleosols interpreted as Entisols and Inceptisols were probably developed in the more proximal portions of the system (i.e., closer to fluvial or tidal channels or to the estuary shoreline), where pedogenesis occurred for shorter amounts of time.

The constructional coalesced deltaic system found along the southwestern to west-central coast of present-day Colombia in the Nariño, Cauca, and Valle del Cauca provinces (Martinez et al. 1995), albeit west facing, can serve as a modern analogue for these environments. This modern coalesced deltaic system has developed along a narrow coastal plain with mountains to the east, and receives yearly precipitation in excess of 150 cm/yr and as high as 800 cm/yr, and sediment yields are higher than the larger watersheds of the Magdalena Valley (Restrepo and Kjerfve 2000). The system is subject to rapid inundation or exposure with minor sea-level oscillation and fresh–seawater mixing is common (Murphy 1939). The majority of soils in the areas of this coastal plain are Entisols, and Inceptisols with minor Ultisols and Histosols (Anonymous 1983).

The $\delta^{18}O$ values for the Caballos Formation are much lighter than the value predicted by extrapolation of the second-order polynomial regression of Ufnar et al. (2002) (Fig. 6). These lighter values highlight the need for improved characterization of groundwater $\delta^{18}O$ over a broad range of latitudes in order to properly define an isotopic gradient for the mid-Cretaceous, or any other time slice. Groundwater values calculated from MSLs are similar to, though slightly more positive than, estimated modern values of precipitation falling over fluvial estuarine systems in the western coast of South America in both the northern and southern hemispheres such as the complex deltaic–estuarine system in the Gulf of Guayaquil, Ecuador (~ 2.2° S), and the coalesced deltaic system of western Colombia (~ 2–4° N). Using the Oxygen Isotopes in Precipitation Calculator—OIPC (Bowen 2009; Bowen and Revenaugh 2003; www.

TABLE 3.—*Isotopic compositions of meteoric water calculated from MSLs.*

Core	Horizon	MSL $\delta^{18}O$ (average VPDB)	Meteoric Water $\delta^{18}O$ (VSMOW)
Los Mangos 4	957.38 m (3141.00 ft)	−4.75‰	−4.90‰
	957.61 m (3141.75 ft)	−3.91‰	−4.06‰
	959.77 m (3148.85 ft)	−3.92‰	−4.07‰
Santa Clara 2	799.01 m (2621.42 ft)	−4.32‰	−4.51‰
	799.15 m (2621.88 ft)	−4.60‰	−4.75‰
	799.22 m (2622.11 ft)	−4.55‰	−4.70‰
San Francisco 52	861.82 m (2827.50 ft)	−4.39‰	−4.54‰
	864.28 m (2835.58 ft)	−4.70‰	−4.85‰
	864.51 m (2836.33 ft)	−5.23‰	−5.38‰
	867.23 m (2845.25 ft)	−4.17‰	−4.32‰
	867.32 m (2845.54 ft)	−4.32‰	−4.47‰
	871.75 m (2860.08 ft)	−4.48‰	−4.63‰
	873.18 m (2864.75 ft)	−3.96‰	−4.11‰

waterisotopes.org) precipitation $\delta^{18}O$ values over these systems are estimated at −5.0 ± 0.6‰ VSMOW. The oxygen isotopic composition of precipitation calculated from Caballos Formation sphaerosiderites is also only slightly more positive than values generated by recent GCM simulations by Poulsen et al. (2007) that calculated precipitation $\delta^{18}O$ values of lower than −5‰ (VSMOW) for this area of Colombia. These consistencies suggest that the oxygen isotopic compositions of MSLs accurately represent the isotopic composition of precipitation at this paleolatitude during the mid-Cretaceous.

While the MSLs from the Caballos Formation show significant consistency in their isotopic composition, two samples have offset compositions. The Los Mangos 4 core at horizon 959.93 m contains sphaerosiderites with variable and more negative $\delta^{18}O$ values and consists of well-formed radial-fibrous crystallites. Though particularly cloudy, the sphaerosiderites do not appear to have been diagenetically altered. Preliminary cathodoluminescence images also show no obvious evidence of late diagenesis. The sphaerosiderites at this horizon are immediately underlain by sandstone approximately 3 meters thick. Pore fluids flowing through this sandstone might have been sourced from isotopically lighter regional aquifers. Study of carbonate cements and sphaerosiderites in the Dakota Formation (Nebraska and Iowa region) by Phillips et al. (2007) indicate that high-altitude precipitation runoff influenced regional aquifers and that this signal was recorded only in the isotopic composition of early-cemented sandstones. Phillips et al. (2007) suggest that the sphaerosiderites, found in paleosols of the interfluvial portions of the estuary to coastal plain environments, captured the local lowland precipitation and were unaffected by the high altitude and isotopically lighter runoff.

The lighter composition of the siderite-cemented sandstone from the San Francisco 52 core at horizon 893.73 m is possibly reflecting diagenetic alteration or at least a very different cementation history. CL images of this sample show a more complicated cement history with common, though small calcite domains. Pore spaces are also filled with silica cement. Furthermore, these siderites are sparry in nature rather than the radial bladed to fibrous crystals of sphaerosiderites in the paleosols. The petrographic observations coupled with the depleted $\delta^{18}O$ values suggest a difference in the pore fluids from which these siderites were precipitated.

During the Aptian, South America and Africa had not completely separated and the Atlantic Ocean was likely not a significant source of water vapor for South America. The Cretaceous Colombian Basin was a southwest–northeast-trending basin open to the proto-Caribbean (Villamil et al. 1999) with sea-surface (i.e., wind-driven) currents bringing waters into the basin from the proto-Caribbean (Johnson 1999). While Johnson (1999) admitted the difficulty of transporting proto-Caribbean waters southward across the equator, it is possible that seasonal deflections of the intertropical convergence zone over the South American continent could have produced wind-driven surface currents that transported proto-Caribbean waters into the basin. This deflection would most likely result in proto-Caribbean-sourced air masses moving over the Guyana Shield and the Cretaceous Colombian Basin. Hence, the major source of precipitation over the Guyana Shield, which at this time drained westward (Potter 1997; Ostos et al. 2005), and over the Cretaceous Colombian Basin, was the proto-Caribbean (Tethys). Thus, the precipitation falling on the fluvio-estuarine depositional settings inferred for the Caballos Formation was most likely a combination of water vapor sourced from the adjacent sea and the proto-Caribbean.

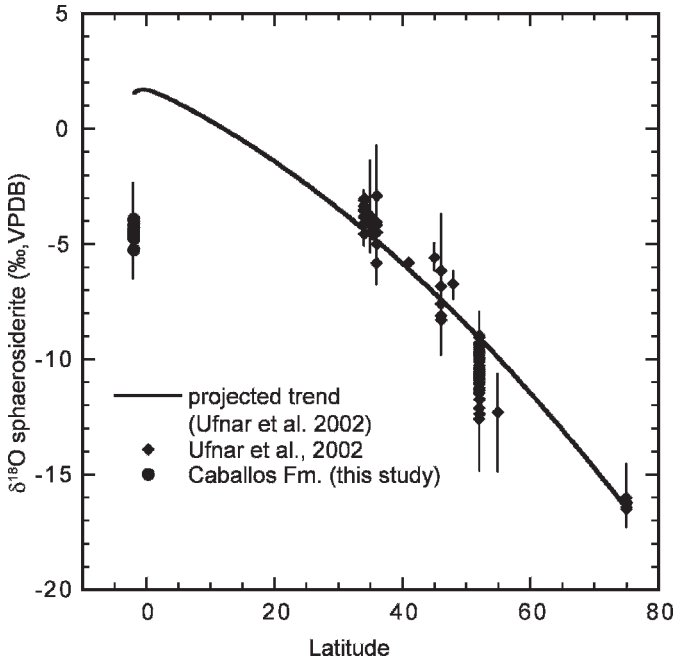

FIG. 6.—Latitudinal variation of sphaerosiderite $\delta^{18}O$ values from the early Late Cretaceous. Each point represents the average of a single horizon. Vertical lines depict the range of all analyses. The curve is fitted to the average $\delta^{18}O$ value at each latitude.

Johnson et al. (1996) proposed that during the late Early Cretaceous (i.e., Aptian–Albian), the Tethys seaway was superheated, and indeed other geologic data suggest intense evaporation in the tropics (Ziegler et al. 2003). Thus, evaporation in the proto-Caribbean would have resulted in localized ^{18}O enrichment of sea-surface water to produce values heavier than −1.2‰. Indeed modeled precipitation $\delta^{18}O$ by Poulsen et al. (2007) shows the proto-Caribbean region precipitation as having slightly heavy isotopic compositions ranging from −3 to −4‰, similar to the compositions calculated for the Caballos Formation MSLs.

CONCLUSIONS

Macroscopic and microscopic features of paleosols in the Caballos Formation in Colombia suggest water-saturated soil conditions during the Cretaceous. Paleosols resemble modern Entisols, Inceptisols, and Ultisols, which also occur in coastal tropical regions of modern Colombia. Isotopic compositions of sphaerosiderites in the paleosols produce meteoric sphaerosiderite lines (MSLs) in $\delta^{18}O$ vs. $\delta^{13}C$ space. The average oxygen isotopic composition of the MSLs from the Caballos Formation is −4.41 ± 0.37‰ (VPDB), which is more negative (by ~ 5‰) than projected values based on data from higher latitudes presented by Ufnar et al. (2002). The latitudinal trend for isotopic

compositions of siderites presented by Ufnar et al. (2002) was not necessarily meant to be characteristic of all latitudes; however, the projected difference between the trend of Ufnar et al. (2002) and the revised trend presented here highlights the necessity of having a more complete latitudinal record of oxygen isotopic data. Using mean annual temperature estimates based on leaf physiognomy, the isotopic composition of groundwater, and thus precipitation, is estimated from average MSL values to be $-4.56 \pm 0.38‰$ (VSMOW). These values are slightly more positive than modern precipitation values at similar latitudes, as well as modeled precipitation values for the Cretaceous. It is likely that more isotopically enriched sea-surface waters from the superheated Tethys Seaway (proto-Caribbean) were a significant source to air masses that produced these precipitation values.

ACKNOWLEDGMENTS

The authors wish to acknowledge the cooperation of Litoteca Nacional de Colombia of the Instituto Colombiano de Petróleo (ICP) in providing core descriptions, access to cores, and core samples. Particular thanks to Core Lab Director, Mr. Nestor Quevedo, and core lab manager Mr. Fabio Ortega, who provided invaluable assistance to L. González during visit to the core lab. Dr. Tomas Villamil and former Core Lab Director Mr. Alberto Ortiz-Fernández were instrumental in securing access to the Litoteca. Assistance in sample analyses at the Keck Paleoenvironmental and Environmental Stable Isotope Lab was provided Mr. Greg Cane. Analyses from the Paul H. Nelson Stable Isotope Laboratory were carried out by Jeremy Davis with assistance of Dr. Scott Carpenter. The manuscript was greatly improved by insightful revisions and edits by Drs. Neil Tabor, Gabriel Bowen, Nathan Sheldon, Paul McCarthy, and John Southard. This study was supported by National Science Foundation grant EAR-0325072 to González and Ludvigson.

REFERENCES

Acevedo, H., and Pennington, W.D., 2003, Porosity and lithology prediction at Caballos Formation at the Puerto Colon oil field in Putumayo (Colombia): The Leading Edge, v. 22, p. 1135–1141.

Allan, J.R., and Matthews, R.K., 1977, Carbon and oxygen isotopes as diagenetic and stratigraphic tools: Surface and subsurface data, Barbados, West Indies: Geology, v. 5, p. 16–20.

Allan, J.R., and Matthews, R.K., 1982, Isotope signatures associated with early meteoric diagenesis: Sedimentology, v. 29, p. 797–817.

Anonymous, 1983, Soil map of Colombia, *in* Selvaradjou, S.-K., Montanarella, L., Spaargaren, O., and Dent, D., eds., 2005 European Digital Archive of Soil Maps (EuDASM)—Soil Maps of Latin America and Caribbean Islands, Luxembourg, Office of the Official Publications of the European Communities, EUR 21822 EN, DVD-Rom version.

Barrero, D., Pardos, A., Vargas, C.A., and Martínez, J.F., 2007. Colombian Sedimentary Basins: Nomenclature, boundaries, and petroleum geology, a new proposal: Bogota, Colombia, Agencia Nacional de Hidrocarburos, 92 p.

Barron, E.J., and Moore, G.T., 1994, Climate Model Application in Paleoenvironmental Analysis: SEPM, Short Course 33, 339 p.

Barron, E.J., Hay, W.W., and Thompson, S., 1989, The hydrologic cycle: A major variable during Earth History: Palaeogeography, Palaeoclimatology, Palaeoecology, v. 75, p. 157–174.

Birkeland, P.W., 1999. Soils and Geomorphology: New York, Oxford University Press, 430 p.

Bowen, G.J., 2009, The Online Isotopes in Precipitation Calculator, version 2.2: http://www.waterisotopes.org.

Bowen, G.J., and Revenaugh, J., 2003, Interpolating the isotopic composition of modern meteoric precipitation: Water Resources Research, v. 39,1299, doi: 10.129/2003WR002086.

Brewer, R., 1964. Fabric and Mineral Analysis of Soils: New York, John Wiley & Sons, 470 p.

Carothers, W.W., Adami, L.H., and Rosenbauer, R.J., 1988, Experimental oxygen isotope fractionation between siderite-water and phosphoric acid liberated CO2-siderite: Geochimica et Cosmochimica Acta, v. 52, p. 2445–2450.

Corrigan, H., 1967, Guidebook to the Geology of the Upper Magdalena Basin (Northern Portion): Colombian Society of Petroleum Geologists and Geophysicists, 41 p.

Curtis, C.D., and Coleman, M.L., 1986, Controls on the precipitation of early diagenetic calcite, dolomite and siderite concretions in complex depositional sequences, *in* Gautier, D.L., ed., Roles of Organic Matter in Sediment Diagenesis, SEPM, Special Publication 38, p. 23–33.

Ecopetrol-ICP, 1999, Registro de Descripción Sedimentologíca y Estratigráfica, Santa Clara 2.

Ecopetrol-ICP, 2000a, Registro de Descripción Sedimentológica y Estratigráfica, Los Mangos 4.

Ecopetrol-ICP, 2000b, Registro de Descripción Sedimentológica y Estratigráfica, San Francisco 52.

Gautier, D.L., and Claypool, G.E., 1984, Interpretation of methanogenic dagenesis in ancient sediments by analogy with processes in modern diagenetic environments, *in* McDonald, D.A., and Surdam, R.C., eds., Clastic Diagenesis, American Association of Petroleum Geologists, Memoir 37, p. 111–123.

Guerrero, J., 2002, A proposal on the classification of systems tracts: application to the allostratigraphy and sequence stratigraphy of the Cretaceous Colombian Basin. Part 2: Barremian to Maastrichtian: Geologia Colombia, v. 27, p. 27–49.

Guerrero, J., Sarmiento, G., and Navarrete, R., 2000, The stratigraphy of the W side of the Cretaceous Colombian Basin in the Upper Magdalena Valley. Reevaluation of selected areas and type localities including Aipe, Guaduas, Ortega, and Piedras: Geologia Colombia, v. 25, p. 45–110.

Hay, W.W., and Deconto, R.M., 1999, Comparison of modern and Late Cretaceous meridional energy transport and oceanology, *in* Barrera, E., and Johnson, C.C., eds., Evolution of the Cretaceous Ocean–Climate System, Geological Society of America, Special Paper 332, p. 283–300.

Heese, R., 1999, Early diagenetic pore water/sediment interaction, *in* McIlreath, I.A., and Morrow, D.W., eds., Diagenesis, Geoscience Canada, Reprint Series 4, p. 277–316.

Jenkyns, H.C., Forster, A., Schouten, S., and Sinninghe Damste, J.S., 2004, High temperatures in the Late Cretaceous Arctic Ocean: Nature, v. 432, p. 888–892.

Johnson, C.C., 1999, Evolution of Cretaceous surface current circulation patterns, Caribbean and Gulf of Mexico, *in* Barrera, E., and Johnson, C.C., eds., Evolution of the Cretaceous Ocean–Climate System, Geological Society of America, Special Paper 332, p. 329–343.

Johnson, C.C., Barron, E.J., Kauffmann, E.G., Arthur, M.A., Fawcett, P.J., and Yasuda, M.K., 1996, Middle Cretaceous reef collapse linked to ocean heat transport: Geology, v. 24, p. 376–380.

Lohmann, K.C., 1988, Geochemical patterns of meteoric diagenetic systems and their application to studies of paleokarst, *in* James, N.P., and Choquette, P.W., eds., Paleokarst: New York, Springer, p. 58–80.

Ludvigson, G.A., Gonzalez, L.A., Witzke, B.J., Brenner, R.L., and Metzger, R.A., 1996, Diagenesis of iron minerals in the Dakota Formation, *in* Witzke, B.J., and Ludvigson, G.A., eds., Mid-Cretaceous Fluvial Deposits of the Eastern Margin, Western Interior Basin: Nishnabotna Member, Dakota Formation: Iowa City, Iowa Department of Natural Resources, p. 31–38.

Ludvigson, G., Gonzalez, L.A., Metzger, R.A., Witzke, B.J., Brenner, R.L., Murillo, A.P., and White, T.S., 1998, Meteoric sphaerosiderite lines and their use for paleohydrology and paleoclimatology: Geology, v. 26, p. 1039–1042.

Martinez, J.O., Gonzalez, J.L., Pilkey, O.H., and Neal, W.J., 1995, Tropical barrier islands of Colobmia's Pacific Coast: Journal of Coastal Research, v. 11, p. 432–453.

McCarthy, P.J., and Plint, A.G., 1998, Recognition of interfluve sequence boundaries: integrating paleopedology and sequence stratigraphy: Geology, v. 26, p. 387–390.

McCarthy, P.J., Faccini, U.F., and Plint, A.G., 1999, Evolution of an ancient coastal plain: paleosols, interfluves, and alluvial architecture in a sequence stratigraphic framework, Cenomanian Dunvagen Formation, NE British Colombia, Canada: Sedimentology, v. 46, p. 861–891.

Meschede, M., and Frisch, W., 1998, A plate-tectonic model for the Mesozoic and early Cenozoic history of the Caribbean plate: Tectonophysics, v. 296, p. 269–291.

Murphy, R.C., 1939, The littoral of Pacific Colombia and Ecuador: Geographical Review, v. 291, p. 1–33.

Ostos, M., Yoris, F., and Avé-Lallemant, H.G., 2005, Overview of the southeast Caribbean–South American plate boundary zone, *in* Avé-Lallemant, H.G., and Sisson, V.B., eds., Caribbean–South American Plate Interactions, Venezuela, Geological Society of America, Special Paper 394, p. 53–89.

Phillips, P.L., Ludvigson, G.A., Joeckel, R.M., Gonzalez, L.A., Brenner, R.L., and Witzke, B.J., 2007, Sequence stratigraphic controls on synsedimentary cementation and preservation of dinosaur tracks: example from the Lower Cretaceous, (upper Albian) Dakota Formation, southeastern Nebraska, U.S.A: Palaeogeography, Palaeoclimatology, Palaeoecology, v. 246, p. 367–389.

Potter, P.E., 1997, The Mesozoic and Cenozoic paleodrainage of South America: a natural history: Journal of South American Earth Sciences, v. 10, p. 331–344.

Poulsen, C.J., 2004, A balmy arctic: Nature, v. 432, p. 814–815.

Poulsen, C.J., Pollard, D., and White, T.S., 2007, General circulation model simulation of the $\delta^{18}O$ content of continental precipitation in the middle Cretaceous: a model-proxy comparison: Geology, v. 35, p. 199–202.

Restrepo, J.D., and Kjerfve, B., 2000, Water discharge and sediment load from the western slopes of the Colombian Andes with focus on Rio San Juan: Journal of Geology, v. 108, p. 17–33.

Retallack, G.J., 1997. A Colour Guide to Paleosols: New York, Wiley, 175 p.

Soil Taxonomy, 1999, Soil Taxonomy: A Basic System of Soil Classification for Making and Interpreting Soil Surveys: U.S. Department of Agriculture, 871 p.

Spicer, R.A., and Corfield, R.M., 1992, A review of terrestrial and marine climates in the Cretaceous with implications for modelling the "Greenhouse Earth": Geological Magazine, v. 129, p. 169–180.

Stoops, G., 2003. Guidelines for Analysis and Description of Soil and Regolith Thin Sections: Madison, Wisconsin, Soil Science Society of America, 184 p.

Suarez, M.B., Gonzalez, L.A., Ludvigson, G.A., Vega, F.J., and Alvarado-Ortega, J., 2009, Isotopic composition of low-latitude paleoprecipitation during the Early Cretaceous: Geological Society of America, Bulletin, v. 121, p. 1584–1595.

Ufnar, D.F., Gonzalez, L.A., Ludvigson, G.A., Brenner, R.L., and Witzke, B.J., 2001, Stratigraphic implications of meteoric sphaerosiderite $\delta^{18}O$ values in paleosols in the Cretaceous (Albian) Boulder Creek Formation, NE British Colombia Foothills, Canada: Journal of Sedimentary Research, v. 71, p. 1017–1028.

Ufnar, D.F., Gonzalez, L.A., Ludvigson, G.A., Brenner, R.L., and Witzke, B.J., 2002, The mid-Cretaceous water bearer: isotope mass balance quantification of the Albian hydrologic cycle: Palaeogeography, Palaeoclimatology, Palaeoecology, v. 188, p. 51–71.

Ufnar, D.F., Gonzalez, L.A., Ludvigson, G.A., Brenner, R.L., and Witzke, B.J., 2004, Evidence for increased latent heat transport during the Cretaceous (Albian) greenhouse warming: Geology, v. 32, p. 1049–1052.

Ufnar, D.F., Ludvigson, G.A., Gonzalez, L.A., and Grocke, D.R., 2008, Precipitation rates and atmospheric heat transport during the Cenomanian greenhouse warming in North America: estimates from a stable isotope mass-balance model: Palaeogeography, Palaeoclimatology, Palaeoecology, v. 266, p. 28–38.

Vegara, S.L., 1995, Organic geochemical data from the Caballos Formation, Upper Magdalena Valley, Colombia: Revista Latino-Americana de Geoquímica Orgánica (ALAGO), v. 1, p. 46–52.

Villamil, T., Arango, C., and Hay, W.W., 1999, Plate tectonic paleoceanographic hypothesis for Cretaceous source rocks and cherts of northern South America, *in* Barrera, E., and Johnson, C.C., eds., Evolution of the Cretaceous Ocean–Climate System, Geological Society of America, Special Paper 332, p. 191–202.

White, T.S., Witzke, B.J., Ludvigson, G.A., Brenner, R.L., Gonzalez, L.A., and Ravn, R.L., 2000, The paleoclimatological significance of Albian (mid-Cretaceous) sphaerosiderites from eastern Saskatchewan and western Manitoba, summary of investigations 2000: Saskatchewan Geological Survey Miscellaneous Report 2000-4.1, v. 1, p. 63–75.

White, T., Gonzalez, L., Ludvigson, G., and Poulsen, C., 2001, Middle Cretaceous greenhouse hydrologic cycle of North America: Geology, v. 29, p. 363–366.

Wolfe, J.A., and Upchurch, G.J.R., 1987, North American nonmarine climates and vegetation during the Late Cretaceous: Palaeogeography, Palaeoclimatology, Palaeoecology, v. 61, p. 31–77.

Ziegler, A.M., Eshel, G., Mcallister Rees, P., Rothfus, T.A., Rowley, D.B., and Sunderlin, B., 2003, Tracing the tropics across land and sea: Permian to present: Lethia, v. 36, p. 227–254.

Received 14 July 2009; accepted 12 January 2010.